

π^- -Meson Production in 2.9-BeV p - p Collisions*

A. C. MELISSINOS, T. YAMANOUCHI, AND G. G. FAZIO

Department of Physics and Astronomy, The University of Rochester, Rochester, New York

AND

S. J. LINDENBAUM AND L. C. L. YUAN

Brookhaven National Laboratory, Upton, New York

(Received July 17, 1962)

Detailed measurements of the production of charged π mesons in proton-proton collisions are reported. The observed results are compared with the "isobar" and "one-pion exchange" models and for single production are in agreement if only the "resonant" part of the π - p cross section is used and if the angular distribution $\cos^6 \theta$ is introduced for the production of the N_1^* isobar. The effects of higher resonances are also considered.

I. INTRODUCTION

THE present experiment is a contribution to the study of the inelastic nucleon-nucleon interaction. The main objective was to investigate the production of charged π mesons in proton-proton collisions using counter techniques. It was possible to measure the π^+ and π^- energy spectra at four c.m. angles with a resolution of the order of 2-4%, and at a proton energy of 2.85 BeV. Preliminary results of the present work were reported in a previous communication.¹

Two other experiments have been performed recently at the same energy and investigated the same basic interaction; one used the BNL 20-in. H_2 bubble chamber^{2,3} and the other measured the recoil proton spectra^{4,5} with counter techniques. All three experiments are in agreement and lead to the conclusion that at this energy the inelastic processes are dominated by the $T=3/2, J=3/2$ π - p resonance and that the angular distribution is highly peaked forward-backward.

From the theoretical models that have been proposed, both the "isobar"⁶ and the "one-pion exchange"⁷ are successful in interpreting the general behavior of some, but not all, of the details of the experimental observations.

Some data useful to the design of secondary π -meson beams at "Cosmotron" energies are also presented.

II. EXPERIMENTAL ARRANGEMENT**A. Beam Optics**

This experiment was performed in the external proton beam III of the "Cosmotron" at the Brook-

haven National Laboratory.⁸ The beam intensity at the second focus was of the order of 30% of the circulating beam (2×10^{10} – 2×10^{11}) and spread over an elliptical area of 1 in. \times 2.5 in.

A 20-in. liquid H_2 target was used; it could be viewed by four channels located at 0°, 17°, 32°, and 45°, respectively (Fig. 1). Each secondary beam channel consisted of an 8 in. \times 32 in. focusing quadrupole doublet and a bending magnet. In general, no slits were used in front of the bending magnets but instead advantage was taken of the properties of the quadrupoles, which were adjusted to focus an image of the target at the defining counter. The calculated resolution curve for a target 1 in. wide and a detector 1.5 in. wide is given in Fig. 2 for the 32° channel. Due to the length of the target it was necessary to limit its apparent width perpendicular to the secondary beam direction to reasonable values; this was achieved by placing a 1 in. \times 4 in. \times 1 in. steel collimator in front of the first quadrupole, for the 17°, 32°, and 45° cases.

The bending magnets were calibrated by the floating wire method. It is not, however, possible to use this technique to determine the quadrupole settings. The quadrupoles were "tuned" during the actual experiment, by maximizing the intensity of transmitted particles at some value of the momentum; a linear relationship in excitation current vs momentum was then used for all other values. In the cases the quadrupoles provided large gains in solid angle (as, e.g., in the 0° beam) the tuning was, in general "sharp"; however, this has the serious drawback, when a production spectrum is measured, that minor errors in quadrupole current setting result in serious errors in counting rate. On the other hand, "flat" tuning, as when part of the quadrupole aperture is masked by a collimator does not suffer from this difficulty.

In order to obtain absolute cross sections, a knowledge of the solid angle and momentum resolution is required. Since the presence of quadrupoles modifies these quantities, yet leaves the relative shape of the spectrum unaltered, several points were measured with quadru-

* This work was supported by the U. S. Atomic Energy Commission.

¹ A. Melissinos, G. Fazio, T. Yamanouchi, S. Lindenbaum, and L. Yuan, *Phys. Rev. Letters* **7**, 12 (1961).

² G. Smith, H. Courant, E. Fowler, H. Kraybill, J. Sandweiss, and H. Taft, *Phys. Rev.* **123**, 2160 (1961).

³ E. Hart, R. Louttit, D. Luers, T. Morris, W. Willis, and S. Yamamoto, *Phys. Rev.* **126**, 747 (1962).

⁴ G. Chadwick, G. Collins, C. Schwartz, A. Roberts, S. DeBenedetti, N. Hien, and P. Duke, *Phys. Rev. Letters* **4**, 611 (1960).

⁵ G. Chadwick, G. Collins, P. J. Duke, T. Fujii, N. Hien, A. Kemp, and F. Turkot, *Phys. Rev.* **128**, 1823 (1962).

⁶ S. J. Lindenbaum and R. M. Sternheimer, *Phys. Rev.* **105**, 1874 (1957).

⁷ F. Selleri, *Phys. Rev. Letters* **6**, 64 (1961).

⁸ G. Piccioni, D. Clark, R. Cool, G. Friedlander, and D. Kassner, *Rev. Sci. Instr.* **26**, 232 (1955).

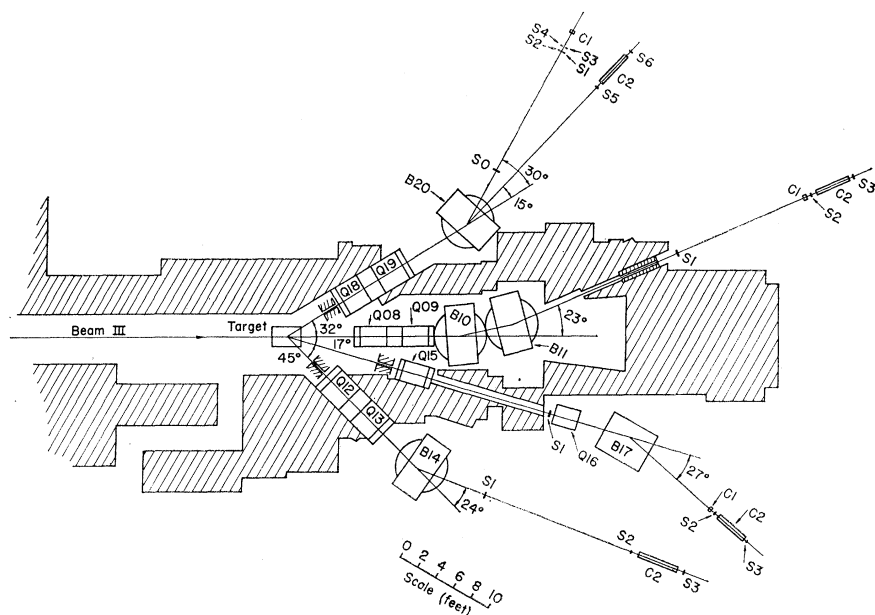


FIG. 1. The experimental setup.

poles off; the experimental spectrum was then normalized to these points. The solid angle was calculated and the momentum resolution was partly calculated, partly taken from the wire measurements. Finally, the length of target viewed through the channel must also be known; this was obtained from the known geometry of the collimator and defining counter.

B. Detectors

In the present experiment the π mesons were detected with scintillation and Čerenkov counters, arranged in a

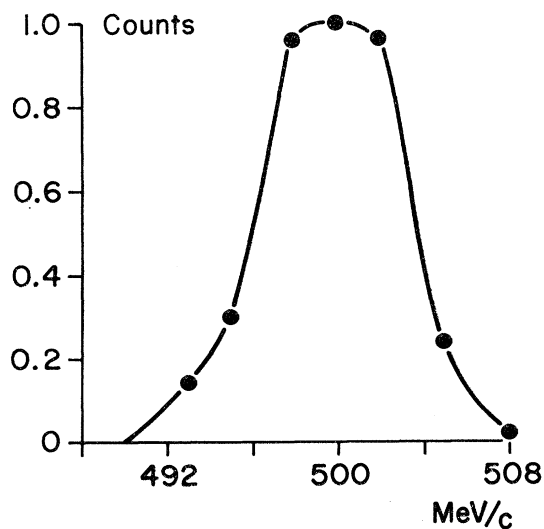


FIG. 2. The calculated momentum resolution (transmission) curve of the 32° channel for proper quadrupole magnet setting. $\Delta\Omega = 3 \times 10^{-3}$ sr, $m_x = -1.60$, $m_y = -3.95$, and $\Delta d\Omega/d\Omega \approx dm/m \approx \frac{1}{10}(\Delta p/p)$.

telescope. Different combinations were used for each channel since the laboratory momentum varies considerably. The secondary beams consist, in general, of π mesons, μ mesons, and electrons; the latter two types of particles can be considered as contaminations. However, in the case of π^+ mesons the channel contains, (predominantly at certain momenta) protons. The selection of the π^+ mesons from the protons was achieved, in general, (i) up to 800 MeV/c by time of flight separation (Fig. 3), (ii) between 600–1000 MeV/c by using a water Čerenkov counter, and (iii) above 850 MeV/c by using a gaseous SF₆ Čerenkov counter⁹; a pressure curve for this counter is shown in Fig. 4.

The scintillation counters were made of plastic polystyrene $\frac{1}{2}$ in. thick and all used R.C.A. 6810A photomultipliers. The electronics were of the standard transistorized Brookhaven design.¹⁰ The performance of the circuits was extremely reliable and their resolution is of the order of 5×10^{-9} sec; thus, the accidental rates were, in general, of negligible value.

Nuclear absorption and multiple scattering in the detectors are considerable, especially in the gaseous Čerenkov counter which at full pressure, (290 psi) presents 18 g/cm² of material in the path of the beam. Corrections for these effects are discussed in Sec. III.

The proton beam was monitored with a three-element telescope placed at 90° to the target and calibrated against the activation of a polyethylene foil using the $C^{12}(p,n\beta)C^{11}$ reaction.¹¹ Our scalars were not gated so

⁹ J. H. Atkinson and V. Perez-Mendez, Rev. Sci. Instr. 30, 864 (1959).

¹⁰ R. M. Sugarman, Brookhaven National Laboratory Report BNL-4436, 1959 (unpublished).

¹¹ J. B. Cumming, G. Friedlander, and C. Schwartz, Phys. Rev. 111, 1386 (1958).

that the whole beam with an energy spread of 3% was used. Background rates were obtained regularly by replacing the hydrogen-filled target with a dummy target.

III. EXPERIMENTAL RESULTS

A. General

The positive and negative spectra were measured at all four laboratory angles; errors due to counting statistics in most cases amount only to few percent. For each angle, data from several completely different runs were combined giving a measure of the internal consistency. The empty target (dummy) rates are also only a few percent.

These spectra were corrected for (a) empty target rates, (b) μ -meson and electron contamination, (c) nuclear absorption and multiple scattering, and (d) π -meson decay.

The completely corrected spectra are shown in Fig. 5 where the indicated errors include the estimated uncertainty introduced through the application of corrections (a-d) above. The uncertainty in the momentum scale is less than 5% and the momentum width (resolution) corresponding to each point is of the order 2-3%.

The absolute value of the cross sections is known only to within 15% because of the difficulties inherent in the determination of the momentum resolution and the target width.

B. Corrections

(a) The empty target rates, as measured were subtracted from the data.

(b) The electron (or e^+) contamination was directly measured for all spectra, by operating the gaseous Čerenkov counter at 50 psi which is well below π - or μ -meson threshold but 100% efficient for electrons. As expected, the contamination was large at low momenta

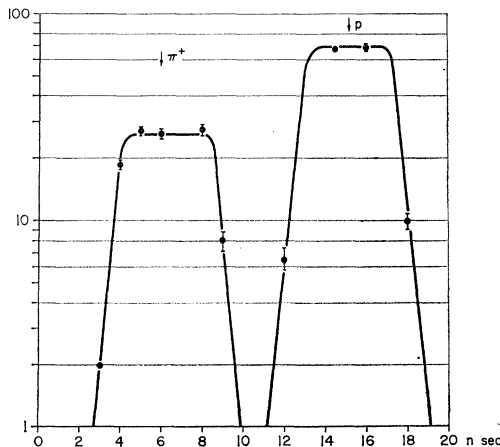


FIG. 3. Time-of-flight separation of 750-MeV/c positive beam; the flight path was 18 ft (expected $\Delta t = 10.5$ nsec). The horizontal scale is in nanoseconds.

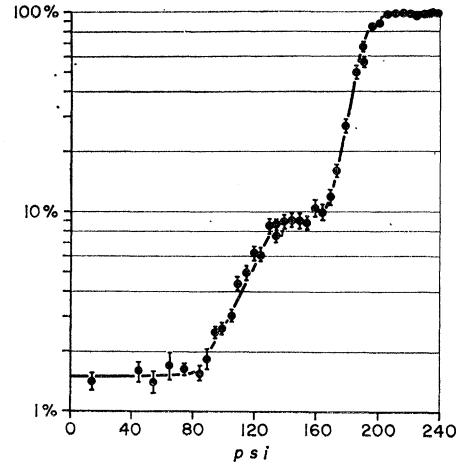


FIG. 4. Counting efficiency vs SF₆ pressure in the gaseous Čerenkov counter for a 920-MeV/c negative beam. Note the e^- , μ^- , and π^- plateau, as well as the final efficiency of the counter.

and reduced to 2% at the high-momentum end; it strongly depended on the beam geometry.

The μ -meson contamination was more difficult to measure. Again the gaseous Čerenkov counter was used, and as is seen in Fig. 4 it is easy to separate the μ mesons from π mesons up to a momentum of the order of 1000 MeV/c; on the other hand, the slowest μ mesons that could be counted (as limited by the highest gas pressure, 290 psi) had a momentum of 650 MeV/c. Therefore, outside this interval we used a calculated value¹² for the μ -meson contamination and normalize our results to the values measured in the 650-1000 MeV/c interval.

(c) The nuclear absorption occurred mainly in the gaseous Čerenkov counter. This effect was measured by taking data with full and with zero gas pressure in the counter; it amounted to 28%. In addition to the nuclear absorption effect, multiple scattering (again mainly in the gaseous counter) was present; this resulted in a momentum dependent correction for particles "scattered out" of the beam. In evaluating the correction reference¹³ was used but data points requiring more than 30% correction were rejected.

(d) The decay correction is straightforward; in view of the considerable length of the flight paths, the cor-

¹² In the calculation we considered contributions to the μ -meson flux from a region inside the collimator and a region external to it. Inside the collimator we assumed equilibrium between π and μ mesons, while outside the collimator only μ mesons arising from the decay of a pion beam are considered. We obtained the formula $N(\mu)/N(\pi)$ (at the detector)

$$= e^{T_2/l_2} (e^{T_1/l_1} - 1) + [(e^{T_1/l_1} - 1) P_C / \pi (\theta l_2)^2],$$

where l_1 is the distance from the target to the collimator and l_2 is the distance from the collimator to the detector; then $T_1 = l_1/\gamma\beta c$, $T_2 = l_2/\gamma\beta c$. θ is the maximum π - μ decay angle which is approximately equal to $30/[\beta\gamma]$ (in MeV/c) and P_C is the area of the collimator (C) projected to the detector, which is of the order of $C(l_1 + l_2)/l_1$. This expression gives the correct limiting behavior of the μ -meson flux and also agrees within small factors with the experimental measurements.

¹³ R. M. Sternheimer, Rev. Sci. Instr. 25, 1070 (1954).

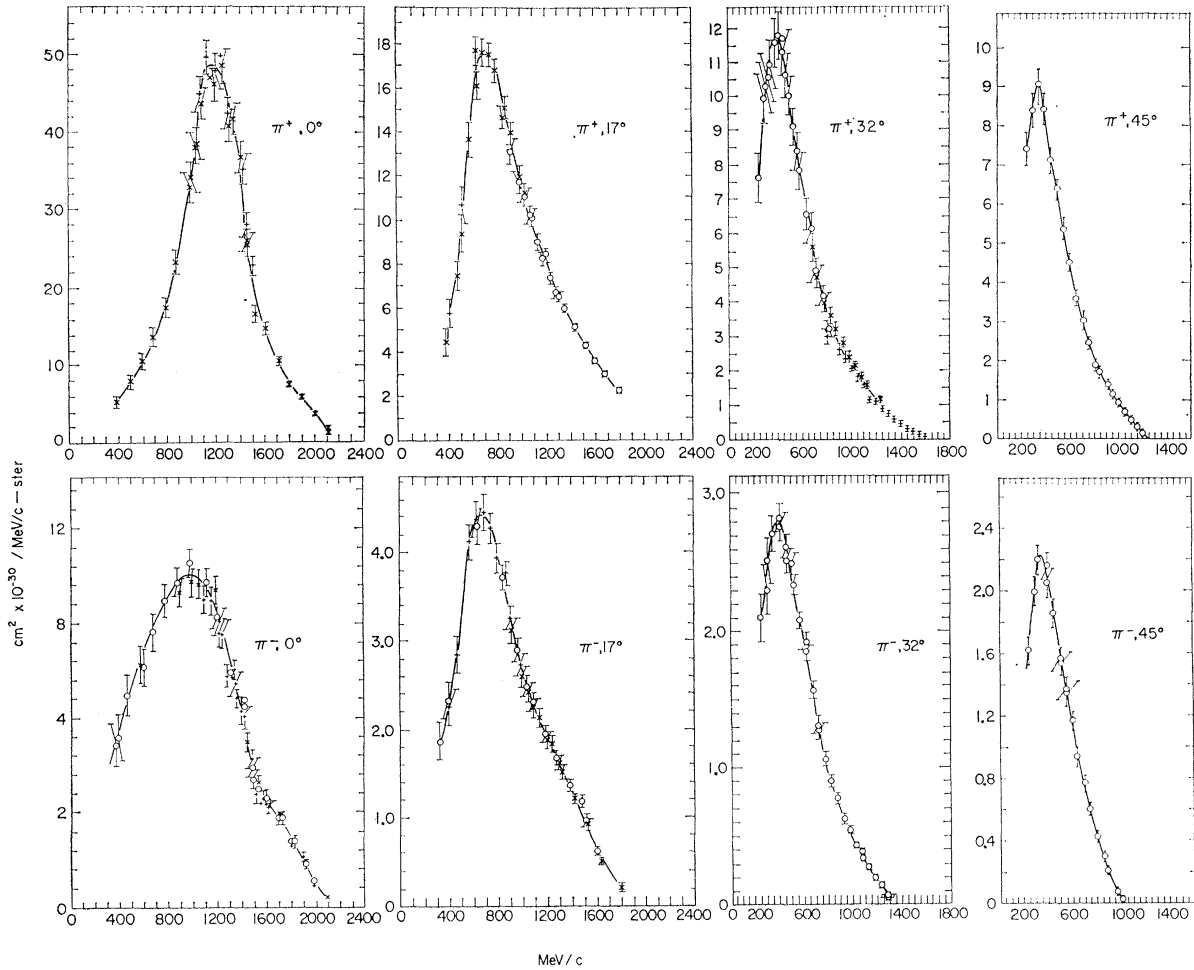


Fig. 5. The laboratory spectrum of π^+ and π^- mesons after the application of all corrections; the flags include all errors introduced through corrections and other systematic sources (excluding absolute calibration).

rection for the lowest momentum was in some channels as high as 80%.

C. π -Meson Production in Carbon

At the 32° channel it was possible to obtain the π -meson spectra from a 2-in.-thick carbon target. They are shown in Fig. 6, and summarized in Table I. As expected, the $\pi^+/\pi^-(C)=2.0$ ratio is smaller in this case than the corresponding one for H_2 (at the same

angle) $\pi^+/\pi^-(H_2)=4.0$. Also the total charged π -meson yield per nucleon is lower in C than in H_2 ; this is due mainly to the increased π^0 production, as well as to nuclear shielding and reabsorption effects.

These results can be used in conjunction with the H_2 data at the other angles, to predict the spectra of π mesons produced by 3-BeV protons on heavy targets.

IV. ANALYSIS OF π -MESON SPECTRA

A. General

The analysis of the experimental spectra of Fig. 5, can be best performed when they are transformed into the c.m. system of the two protons. The transformed spectra are given in Table II and shown on Fig. 7. A marked anisotropy is apparent.

The integrated (over momentum) values of the differential cross section for each angle are given in Table III; these values are used to obtain the angular distribution of π mesons and, hence, a value for the

TABLE I. Differential cross sections in the laboratory system for π -meson production from carbon and hydrogen at 32°.

	$d\sigma/d\Omega \left(\frac{\text{cm}^2 \times 10^{-27}}{\text{sr-nucleon}} \right)$			$R = \pi^+/\pi^-$
	π^+	π^-	$(\pi^+ + \pi^- + \pi^0)$ (estimated)	
Carbon	3.67	1.86	9.2	2.0
Hydrogen	6.48	1.64	11.4	4.0

total cross section. Within experimental error, the total cross sections agree with the results given in references 2 and 3.

Since we consider the p - p system the results must have complete symmetry about 90° in the c.m. system. In this respect the 108° spectrum is indicative of the internal consistency of our data since it must be almost the same as the 83° data. Both Fig. 7 as well as the differential cross sections of Table III indicate that such agreement (within error limits) exists at these angles.

For a proton energy of 2.85 BeV at which this experiment was performed, it is known^{2,3,14,15} that both double and triple production occur with cross sections of the same order as the single production. This is a complica-

TABLE II. Energy spectra in the c.m. system for π^+ mesons produced in H_2 by 2.85-BeV protons at the corresponding c.m. angles.

\bar{T}_π	$\frac{d\sigma}{d\Omega dE}$		$\left(\frac{\text{cm}^2 \times 10^{-30}}{\text{MeV-sr}}\right)$	
	0°	47°	83°	108°
(a) π^+ mesons				
50	(1.6) ^a	(2.0)	4.0	(3.6)
100	(3.4)	4.2	6.1	5.8
150	(5.4)	6.6	5.4	6.7
200	8.9	6.8	4.1	5.7
250	14.0	5.3	3.0	4.5
300	16.5	4.2	2.3	3.6
350	13.0	3.3	1.8	2.7
400	6.8	2.6	1.3	2.0
450	4.0	2.0	1.0	1.5
500	2.8	1.5	0.7	1.2
550	1.5	1.1	0.5	0.9
600	0.6	(0.8)	0.3	0.6
650	0	(0.4)	0.1	0.4
700		0	0	0.2
750				0
800				
(b) π^- mesons				
50	(1.2)	(0.75)	1.05	(0.72)
100	(1.7)	1.45	1.46	1.23
150	2.1	1.7	1.35	1.64
200	2.4	1.55	1.05	1.44
250	2.4	1.2	0.80	1.17
300	2.1	0.95	0.57	0.90
350	1.6	0.75	0.42	0.70
400	1.0	0.65	0.30	0.50
450	0.8	0.45	0.20	0.33
500	0.5	0.30	0.12	0.20
550	0.3	0.20	0.05	0.08
600	0.1	0.07	0	0.02
650	0	0		0
700				
750				

^a Parentheses indicate extrapolated values, rather than direct measurement.

¹⁴ W. Fowler, R. Shutt, A. Thorndike, and L. Whittemore, Phys. Rev. **95**, 1026 (1954).

¹⁵ L. C. L. Yuan and S. J. Lindenbaum, Phys. Rev. **103**, 404 (1956).

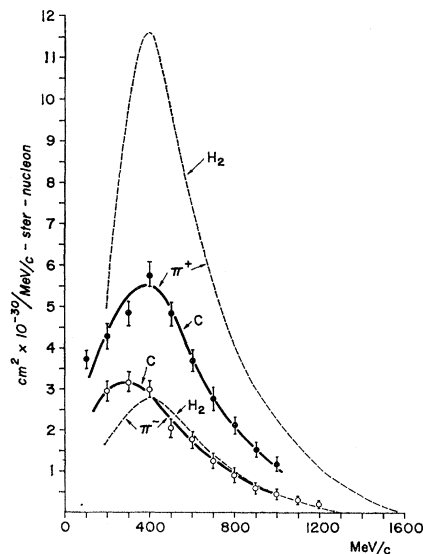


FIG. 6. π^+ - and π^- -meson laboratory spectra produced from carbon nuclei at 32° . For comparison the dashed curves represent the corresponding spectra obtained in hydrogen. In all cases the cross section per nucleon is given.

tion in the analysis of the experimental results since, in the present case, it is not possible to distinguish between the various processes.

In the p - p case, however, all negative π -meson production must occur through the two and three π -meson channels. This fact, then, can be used for obtaining the spectrum for single π^+ -meson production, by making the plausible assumption that the π^+ double- and triple-production spectrum is not much different from the π^- spectrum in the same channels. Details of this subtraction procedure are given in the next paragraph.

The reason for placing so much emphasis on the single production spectrum is that the two theoretical models we are considering can make definite predictions in this case.

The "one-pion exchange" model in its present form¹⁶ predicts both the absolute cross section as well as the angular distribution for the recoil nucleon (and thus of the excited "isobar"); if it is assumed that the isobar

TABLE III. Summary of differential cross sections in the c.m. systems for π^\pm meson production on H_2 by 2.85-BeV protons at the corresponding c.m. angles.

	$\frac{d\sigma}{d\Omega} \left(\frac{\text{cm}^2 \times 10^{-27}}{\text{sr}}\right)$				Angular distribution	$\sigma_t (\text{cm}^2 \times 10^{-27})$	
	0°	47°	83°	108°		Present work	Bubble chamber ^{a,b}
π^+	3.93	2.05	1.55	1.99	$1.6(1 + (2/3)\cos\theta)$	26.1 ± 5	24.6 ± 1.0
π^-	0.82	0.50	0.37	0.45	$0.4(1 + \cos\theta)$	6.0 ± 1.2	4.6 ± 0.2

^a See reference 2.
^b See reference 3.

¹⁶ We would like to thank Dr. F. Selleri for informing us on the progress of a new calculation based on the "one-pion exchange" model which will predict the π -meson spectra.

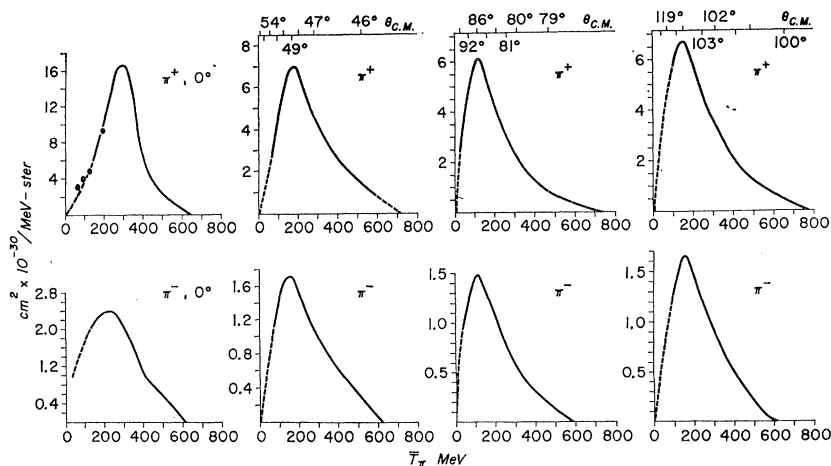


FIG. 7. The c.m. energy spectra in $\mu\text{b}/(\text{MeV}\cdot\text{sr})$ for π^+ and π^- mesons produced at four different laboratory angles; the corresponding c.m. angles are indicated.

decays isotropically in its own rest frame it is possible to obtain the spectrum of the singly produced π^+ or π^0 mesons.¹⁷ The "extended isobar"²¹⁸ model, on the other hand, makes predictions about a large variety of production channels by assuming two isobars N_1^* ($T=3/2$) and N_2^* ($T=1/2$), where N_2^* can decay by two-pion emission via N_1^* . However, one must introduce the relative probabilities for the production of the various combinations of N_1^* and N_2^* which can be determined only from the experimental cross sections for the different production channels. Thus, in spite of the many channels predicted, the crucial test of this model rests mainly with the single-meson spectrum.

The original calculations of the "isobar"¹⁸ were performed for complete isotropy, but one can introduce an angular distribution for isobar production and thus obtain the angular dependence of the π -meson spectra; this method was used in our analysis.

B. π^+ Spectra

As mentioned in the previous paragraph, we attempted to extract the single meson spectrum by a

subtraction technique. The bubble chamber (bbc) data^{2,3} (with which our total cross sections are in agreement) were used to obtain differential cross sections for single meson production ($d\sigma/d\Omega$) (θ ; single bbc), we determine then a multiplicative factor F such that at each angle;

$$\frac{d\sigma}{d\Omega}(\theta; \pi^+ \text{ exper.}) - F \left[\frac{d\sigma}{d\Omega}(\theta; \pi^- \text{ exper.}) \right] = \frac{d\sigma}{d\Omega}(\theta; \text{single bbc}).$$

Details of this procedure and the values of F are given in Table IV. The single spectra were finally obtained by subtracting from the π^+ -meson spectrum the spectrum for π^- mesons multiplied by F . Other procedures for arriving at F , such as branching ratios predicted by the isobar or the total cross sections for each π -meson channel,³ lead to similar values.

The spectra for single π^+ production are shown in Fig. 8 as the heavy curves; (only the three c.m. angles

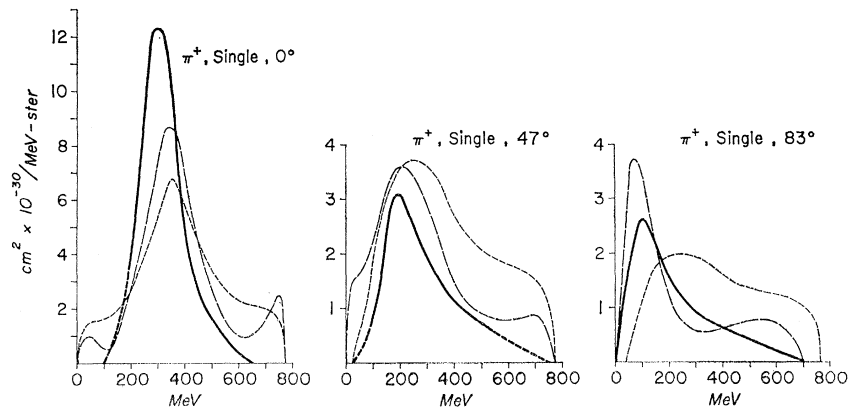


FIG. 8. The c.m. spectra for single π^+ production obtained through the subtraction technique described in the text. The heavy curve gives the experimental results; the dashed (long dashes) curve gives the theoretical predictions of the "isobar model," and the short-dashed curve gives the predictions of the "one-pion exchange" model, using the complete $\pi^+ - p$ cross section. The isobar prediction has been normalized once to fit the area under the experimental curve at 0° ; note that the 47° and 83° vertical scales are expanded two times.

¹⁷ We used, with minor modifications, the 7090 program of N. C. Hen and collaborators.

¹⁸ R. M. Sternheimer and S. J. Lindenbaum, Phys. Rev. **123**, 333 (1961).

TABLE IV. Determination of the subtraction factor for single production spectra (see text).

$\theta_{c.m.}$	Single (bbc) ²	$\frac{d\sigma}{d\Omega} \left(\frac{\text{cm}^2 \times 10^{-27}}{\text{sr}} \right)$	π^+ (exp)	π^- (exp)	F
0°	2.26		3.93	0.82	2.04
47°	0.82		2.05	0.50	2.40
83°	0.68		1.55	0.37	2.35

are used since the fourth one does not add new information). In the same figure are displayed the results of the "one-pion exchange" model (short dash curve) and of the isobar model (long dashes). For the isobar model a $(\cos^{10}\theta)$ angular distribution for isobar production was assumed; the predicted spectrum was normalized to the observed one *only* at 0°. One is immediately forced to use a distribution of this general form because of the large anisotropy in the differential cross sections, which completely excludes the isotropic isobar.

For both models the total cross section for π - p scattering in the $T=3/2$ channel was used (curve I, Fig. 9).¹⁹ This is necessary because it determines the scattering of the virtual pion (exchange model) or the probability for isobar excitation (isobar model). The entire range of isobar masses allowed by the kinematics was used ($m_I=2.06 \text{ BeV}/c^2$).

It is noticed that both models give results of a similar nature. The "one-pion exchange" gives the correct order of magnitude for the cross section, even though at all angles the prediction is not in agreement with the observed spectra. In general, it is difficult to compare the low-momentum behavior, because of the experimental uncertainty; but on the high-momentum side both models predict shoulders (most pronounced in the 0° case) which are definitely *not* observed.

In view of this discrepancy the calculation was repeated for both models but using the modified $T=3/2$

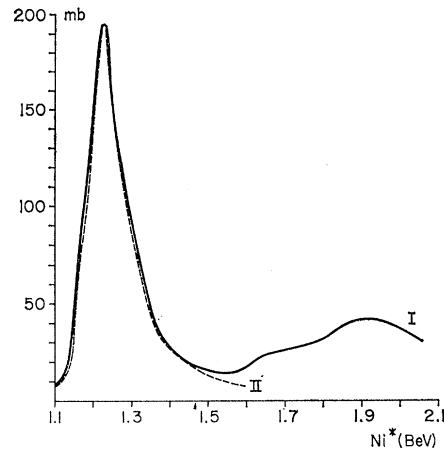


FIG. 9. The π - p total scattering cross section in the $T=3/2$ channel that was used in the theoretical models. Curve I is the complete cross section containing isobar masses up to the kinematical limit of 2.06 BeV; curve III is the "resonant" cross section (cutoff at 1.6 BeV).

π - p scattering cross section shown as curve II in Fig. 9. It essentially consists in applying a cutoff at an isobar mass of 1.6 BeV, namely, in using only what we call the "resonant" part of the $T=3/2$ scattering cross section. The results so obtained are shown in Fig. 10 and the agreement between experiment and theory is much improved. Similar cutoffs have been used by other authors as well.²⁰

Next, a steeper angular distribution for isobar production ($\cos^{10}\theta$) has been introduced, and the resulting π -meson spectra are given by the thin curves in Fig. 11. The theoretical spectra have been normalized only at 0° and a fair agreement between the isobar predictions and experiment is apparent at all three angles.

We can also conclude that the $T=1/2$ state plays a minor, if any, role in single meson production, at these energies.

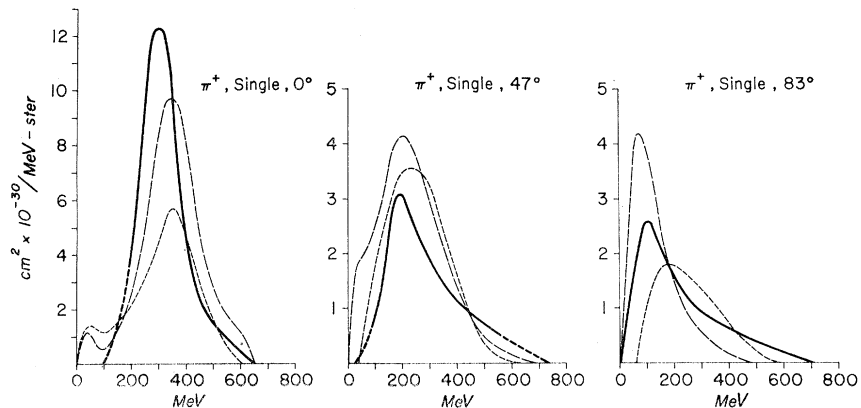


FIG. 10. Same as Fig. 9 above, but only the "resonant" part of the π^+p cross section (curve II Fig. 9) has been used in calculating the theoretical spectra.

¹⁹ T. Devlin, B. Moyer, and V. Perez-Mendez, University of California Radiation Laboratory Report (unpublished) UCRL-9548; S. J. Lindenbaum, Ann. Rev. Nuclear Sci. 7, 317 (1957).

²⁰ E. Ferrari and F. Selleri, Phys. Rev. Letters 7, 387 (1961).

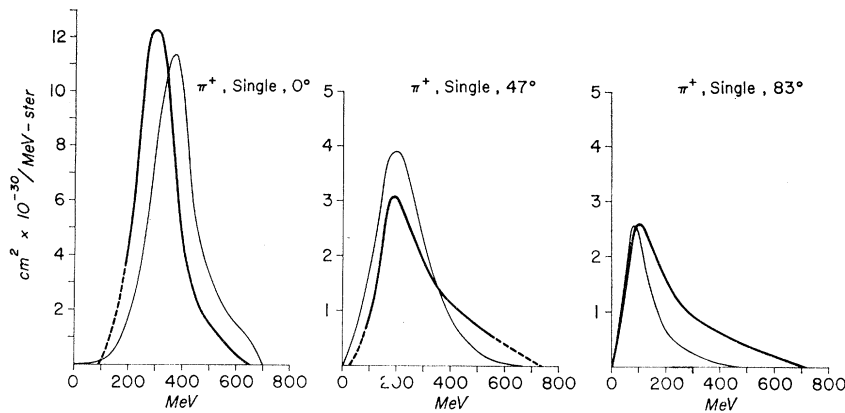


FIG. 11. The experimentally measured c.m. spectra for single π^+ production (heavy curve) compared with the predictions of the "isobar model" (thin curve) when an angular distribution ($\cos^2\theta$) is introduced for isobar production. The theoretical curves have been normalized once to fit the area under the experimental curve at 0° .

C. π^- Spectra

Next we use the π^- -meson spectra to obtain information about the multiple production processes; for this purpose the π^- production is superior to the π^+ , since it is devoid of single production.

By inspection (Figs. 7, 12) it is seen that the angular dependence is much less pronounced than in the π^+ case, even though some anisotropy is still present. Because of the large number of isobar channels that are open, it is futile (and impossible) to make an angle-dependent analysis, as was done for the single spectra. Instead, the predictions of the isotropic isobar have been calculated and are discussed in connection with the 0° spectrum (Fig. 12); obviously the same spectra (isotropy) apply to the other two angles.

For negative meson production at 2.85 BeV the isobar channels that contribute are the following:

- (a) $\frac{1}{5}[N_1^*(T_3=3/2)+N_1^*(T_3=-1/2)] \rightarrow pp+-$,
- (b) $\frac{1}{2}[N_1^*(T_3=3/2)+N_2^*(T_3=-1/2)] \rightarrow pp+-$,
- (c) $(5/9)[N_1^*(T_3=3/2)+N_2^*(T_3=+1/2)] \rightarrow pp+-$,
- (d) $(39/54)[N_1^*(T_3=3/2)+N_2^*(T_3=+1/2)] \rightarrow pp+-$
and pn^{++-} .

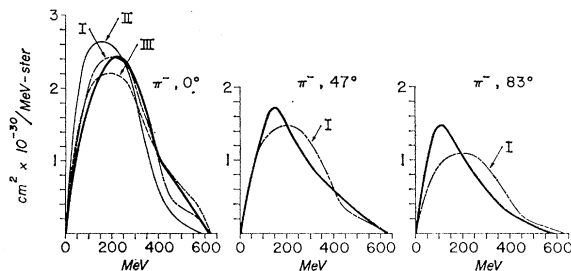


FIG. 12. Center-of-mass spectra for π^- mesons compared with the predictions of the "extended isobar" model. The heavy curves indicate the experimental data. Curve I (dash-dot) is the theoretical curve including all possible channels for π^- production; curve II (thin solid) is the theoretical curve for channel (a) only (see text); curve III (dashed) is the theoretical curve for double production only. In each case the theoretical curves have been normalized separately to the area under the experimental curve.

The numerical factors which are the appropriate Clebsch-Gordan coefficients indicate what portion of the isobar channels (a) through (d) contributes to the π^- -meson channel shown on the right-hand sides. Further, each isobar channel has to be weighed by a relative excitation probability which was obtained from the bubble chamber data^{2,3} (by the inverse procedure); we used

$$\begin{aligned}\sigma(a) &= 8.0 \text{ mb,} \\ \sigma(b) &= 1.0 \text{ mb,} \\ \sigma(c) &= 1.0 \text{ mb,} \\ \sigma(d) &= 2.7 \text{ mb.}\end{aligned}$$

The resulting π^- -meson spectra are shown in Fig. 12 together with the experimental points. Curve I represents the total contribution of channels (a) through (d); curve II, channel (a) only; and curve III, channels (a), (b), and (c). All three curves are normalized to fit the area under the experimental spectrum.

If for 0° , one believes curve III (which implies the relative suppression of triple production in the forward direction), this spectrum may constitute evidence in favor of the creation of the $T=1/2$ isobar, and its contribution to double meson production. At the other two angles only Curve I has been plotted but it is renormalized to the experimental data. However, to account for the smaller differential cross sections and the shift of the peak towards lower energies, one must introduce a different angular distribution for each channel, which we have not attempted to do.

From the π^- -meson data we are led to the conclusion that some anisotropy persists even for double meson production through the N_1^* isobar; this does not exclude the possibility that N_2^* may be produced isotropically.

Finally, in concluding the discussion of the π spectra we would like to mention the sharp break at 410 MeV c.m. energy in the 0° experimental curve. We do not know if this apparent discontinuity is due to a real structure narrower than the resolving power of our apparatus, or whether it is the result of the super-

TABLE V. Data on elastic p - p scattering at 2.85 BeV.
($k_{c.m.} = 5.8 f^{-1}$.)

$\theta_{c.m.}$	$\Delta = 2k \sin(\theta/2) (f^{-1})$	$\frac{d\sigma}{d\Omega} \left(\frac{\text{cm}^2 \times 10^{-27}}{\text{sr}} \right)$
116°	6.15 f^{-1}	0.26 ± 0.07
90°	8.2 f^{-1}	0.065 ± 0.02

position of two broad, but spectrally different contributions to multiple meson production.

V. PROTON SPECTRA

At the two laboratory angles of 32° and 45° the proton spectrum was measured since this region was not covered by other workers.^{4,5} Figure 13 gives the c.m. energy spectra for protons at the corresponding c.m. angles of 90° and 116° (64°).

The elastic scattering peak is clearly defined at both angles, and the relevant data are summarized in Table V. These data are in agreement with the results of Smith *et al.*² and are of the same order of magnitude as the results of Wenzel *et al.*²¹ at a different energy but at the same momentum transfer.

In the inelastic proton spectrum we cannot identify peaks corresponding to recoil protons from isobar formation. The expected position of these peaks associated with N_1^* (1.23 BeV) and N_2^* (1.6 BeV) is indicated in the figure. The 90° (c.m.) spectrum is devoid of any structure within the resolution of our observations while the 64° (c.m.) spectrum gives a slight indication of a shoulder at the position of the 1.23-BeV isobar. This observation is consistent with the results of Chadwick *et al.*^{4,5} and indicates clearly that single N_1^* production is highly inhibited at large c.m. angles.

VI. CONCLUSIONS

In the present work we have been concerned with the production of π mesons in p - p collisions at 2.85 BeV, which lead to both single and multiple production processes. These processes are strongly connected with the π - p scattering cross section and are dominated at this energy (and probably at higher energies too) by the $T=3/2, J=3/2$ resonant state.

The single production process is strongly anisotropic, and can be accurately predicted if one assumes the production of an isobaric nucleon state⁶ with an angular dependence of the type $(\cos^{16}\theta)$ and an excitation func-

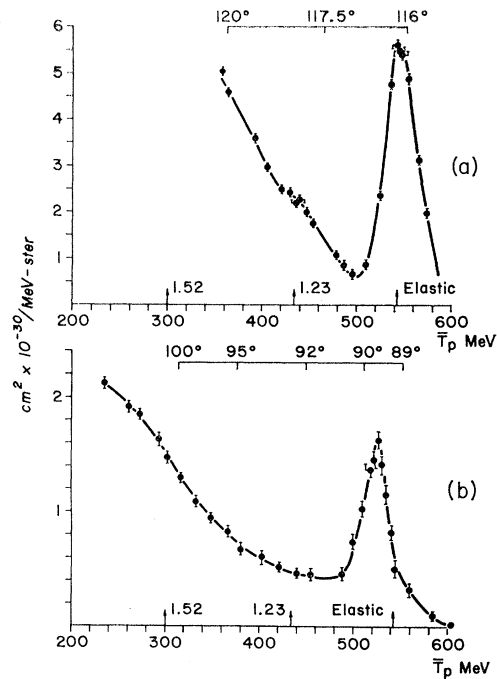


FIG. 13. Center-of-mass spectra of 2.85-BeV protons scattered (a) at 45° in the laboratory, (b) at 32° in the laboratory. The arrows indicate the position of nucleons scattered elastically from protons, from the N_1^* isobar, and from the N_2^* isobar.

tion that includes only the “resonant part” of the $T=3/2$ π - p scattering cross section; (cut off in the vicinity of 1.6 BeV).

The multiple (double and triple) production process shows a slight angular dependence but includes contributions from isobaric states certainly, with $T=3/2$ and, probably, also with $T=1/2$.

The one-pion exchange model in its present form,¹⁷ even though partly successful cannot account for many features of the experimental observations.

Finally, the data for meson production from carbon nuclei are in accord with the data obtained from H_2 .

ACKNOWLEDGMENTS

It is a pleasure to acknowledge the cooperation of the Cosmotron staff, operating crew, and experimental support group, as well as of the members of the University of Rochester 130-in. cyclotron. We also thank S. Weaver for participation in the early stages of this experiment and Dr. N. Hien and collaborators for lending us their 7090 code on the one-pion exchange model. Finally, we would like to thank many other members of the Brookhaven staff for discussions and suggestions.

²¹ B. Cork, W. Wenzel, and C. Causey, Jr., Phys. Rev. **107**, 859 (1957).